MTL TR 92-46

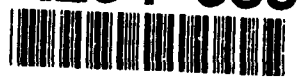

AN INVESTIGATION OF RESIDUAL STRESSES IN MACHINED SILICON NITRIDE

DANIEL J. SNOHA
U.S. ARMY MATERIALS TECHNOLOGY LABORATORY
MATERIALS TESTING AND EVALUATION BRANCH

MICHAEL R. FOLEY
SAINT GOBAIN/NORTON INDUSTRIAL CERAMICS CORPORATION
NORTHBORO, MA

July 1992

US ARMY
LABORATORY COMMAND
MATERIALS TECHNOLOGY LABORATORY

U.S. ARMY MATERIALS TECHNOLOGY LABORATORY
Watertown, Massachusetts 02172-0001

The findings in this report are not to be construed as an official Department of the Army position, unless so designated by other authorized documents.

Mention of any trade names or manufacturers in this report shall not be construed as advertising nor as an official indorsement or approval of such products or companies by the United States Government.

DISPOSITION INSTRUCTIONS

Destroy this report when it is no longer needed.
Do not return it to the originator.

UNCLASSIFIED

SECURITY CLASSIFICATION OF THIS PAGE *(When Data Entered)*

REPORT DOCUMENTATION PAGE		READ INSTRUCTIONS BEFORE COMPLETING FORM
1. REPORT NUMBER MTL TR 92-46	2. GOVT ACCESSION NO.	3. RECIPIENT'S CATALOG NUMBER
4. TITLE *(and Subtitle)* AN INVESTIGATION OF RESIDUAL STRESSES IN MACHINED SILICON NITRIDE		5. TYPE OF REPORT & PERIOD COVERED Final Report 6. PERFORMING ORG. REPORT NUMBER
7. AUTHOR*(s)* Daniel J. Snoha and Michael R. Foley*		8. CONTRACT OR GRANT NUMBER*(s)*
9. PERFORMING ORGANIZATION NAME AND ADDRESS U.S. Army Materials Technology Laboratory Watertown, Massachusetts 02172-0001 SLCMT-MRM		10. PROGRAM ELEMENT, PROJECT, TASK AREA & WORK UNIT NUMBERS
11. CONTROLLING OFFICE NAME AND ADDRESS U.S. Army Laboratory Command 2800 Powder Mill Road Adelphi, Maryland 20783-1145		12. REPORT DATE July 1992 13. NUMBER OF PAGES 20
14. MONITORING AGENCY NAME & ADDRESS *(if different from Controlling Office)*		15. SECURITY CLASS. *(of this report)* Unclassified 15a. DECLASSIFICATION/DOWNGRADING SCHEDULE

16. DISTRIBUTION STATEMENT *(of this Report)*

Approved for public release; distribution unlimited.

17. DISTRIBUTION STATEMENT *(of the abstract entered in Block 20, if different from Report)*

18. SUPPLEMENTARY NOTES

*Saint Gobain/Norton Industrial Ceramics Corporation, Northboro, MA

19. KEY WORDS *(Continue on reverse side if necessary and identify by block number)*

Residual stress	Tensile rods	Integrated intensity
X-ray diffraction	Flexure bars	Full-width half-maximum
Silicon nitride	Reaction layer	

20. ABSTRACT *(Continue on reverse side if necessary and identify by block number)*

(SEE REVERSE SIDE)

DD FORM 1 JAN 73 1473 EDITION OF 1 NOV 65 IS OBSOLETE

UNCLASSIFIED

SECURITY CLASSIFICATION OF THIS PAGE *(When Data Entered)*

Block No. 20

ABSTRACT

An X-ray diffraction (XRD) residual stress investigation was conducted on groups of machined silicon nitride specimens utilizing copper Kα radiation, the (323) β-phase crystallographic planes and the $\sin^2 \psi$ stress-measuring technique. Cylindrical button-head tensile specimens formed by different processes and finish machined by different shops were characterized both before and after heat treatment. Surface machining stresses were also determined on a partial-machined tensile rod and on fractured flexure bars. The residual stress results are presented in the form of a comparative evaluation of processing parameters. Supplemental integrated intensity data from measurements on the partial-machined tensile rod and crushed buttonhead powder samples has demonstrated that XRD residual stress analysis may be applicable as a quality assurance procedure.

CONTENTS

INTRODUCTION

Residual stresses introduced into structural ceramic materials by forming and surface finishing processes can influence the mechanical properties and overall performance of the ceramic component. In an effort to characterize the final stress field on groups of machined NCX-5102 (4% Y_2O_3 doped Si_3N_4) specimens, Saint Gobain/Norton Industrial Ceramics Corporation (SG/NICC, formerly Norton Company), Northboro, MA requested the U.S. Army Materials Technology Laboratory (MTL) perform X-ray diffraction residual stress analysis. It was, therefore, the primary objective of this investigation to quantify, for comparative purposes, surface residual stresses in the gage region on finish-machined cylindrical buttonhead tensile specimens produced by three uniquely distinct forming processes and machined by three different shops, and to determine the effect of heat treatment on the magnitude of these stresses. A partial-machined tensile rod, fractured flexure bar specimens, and crushed buttonhead powder samples were similarly tested. This report is a compilation of residual stress measurement results from four approximately one-week long test service programs conducted at MTL during the period April 1990 through December 1991.

Thirteen cylindrical buttonhead tensile specimens, 14 fractured flexure bars, and two crushed buttonhead powder samples were received at MTL and are identified in Table 1 along with the forming process, machine shop utilized, and the condition of the surface tested. SG/NICC provided as-formed tensile rods to the three machine shops with specifications for producing finish-machined cylindrical buttonhead tensile specimens. After rough machining with a 180 grit diamond wheel, the tensile rods were finish machined in the axial direction with a 320 grit diamond wheel to a final gage region diameter of 6.35 mm (0.25"). An engineering drawing (in inches) and photograph of a finish-machined tensile rod specimen shown in Figure 1 provides dimensional reference and indicates locations and directions of residual stress measurement. The fractured flexure bars conformed to ASTM Standard C1161-90 (Flexural Strength of Advanced Ceramics at Ambient Temperature), Type B (3 mm x 4 mm cross section), and were nominally 27.1 mm (1.07") in length. And the powder samples were prepared by crushing the buttonheads of a finish-machined tensile rod then passing the particles through a 325-mesh screen.

Methodologies for the experimental determination of residual stress include Barkhausen noise analysis (magnetoelastic interaction); ultrasonic (acoustic wave propagation); hole drilling, cut and section, and compliance (mechanical relaxation); and neutron and X-ray diffraction.[1-6] The nondestructive, noncontact X-ray diffraction method has found widespread application and is generally accepted as being the most accurate of these techniques.

1. RUUD, C. O. *A Review of Selected Non-Destructive Methods for Residual Stress Measurement.* NDT Intl., v. 15, no. 1, February 1982, p. 15-22.
2. *Determining Residual Stresses by the Hole-Drilling Strain-Gage Method.* ASTM Standard E 837-89.
3. CHENG, W., and FINNIE, I. *Measurement of Residual Hoop Stresses in Cylinders Using the Compliance Method.* J. Eng. Mater. and Tech., v. 108, April 1986, p. 87-92.
4. ROY, G., and KIFF, D. *Determination of Residual Stress State in Single-Pass Weldment.* CANMET/MTL 86-93, Ottawa, Ontario, Canada, 1986.
5. KRAWITZ, A. D., and HOLDEN, T. M. *The Measurement of Residual Stresses Using Neutron Diffraction.* MRS Bul., November 1990, p. 57-64.
6. *Residual Stress Measurement by X-Ray Diffraction - SAE J784a.* Soc. of Auto. Eng., Warrendale, PA, 1971.

Table 1. SG/NICC NCX-5102 SILICON NITRIDE SPECIMENS

Specimen ID	Forming Process	Machine Shop	Surface Condition
Tensile Rods			
1, 2, 3, 4	Cold Isostatic Pressed Hot Isostatic Pressed	A	Finish Machined
I27, I36	Injection Molded, HIP	A	Finish Machined
D71	IM, HIP	N/A	As-HIPed
NL, NT	Pressure Cast, HIP	A	Finish Machined
N18, NI	PC, HIP	B	Finish Machined
NV	PC, HIP	C	Finish Machined
R16	PC, HIP	A	Partial Machined
Flexure Bars			
C005 16, 22, 44	CIP, HIP	A	Finish Machined
C006 15, 22, 38, 44			
C007 16, 22, 38, 44			
C008 16, 22, 43			
Powder Samples			
T-end, 1-end	N/A	N/A	N/A

Shop A: SG/NICC, Northboro, MA B: Eonic, Detroit, MI C: Chand/Kare, Worcester, MA

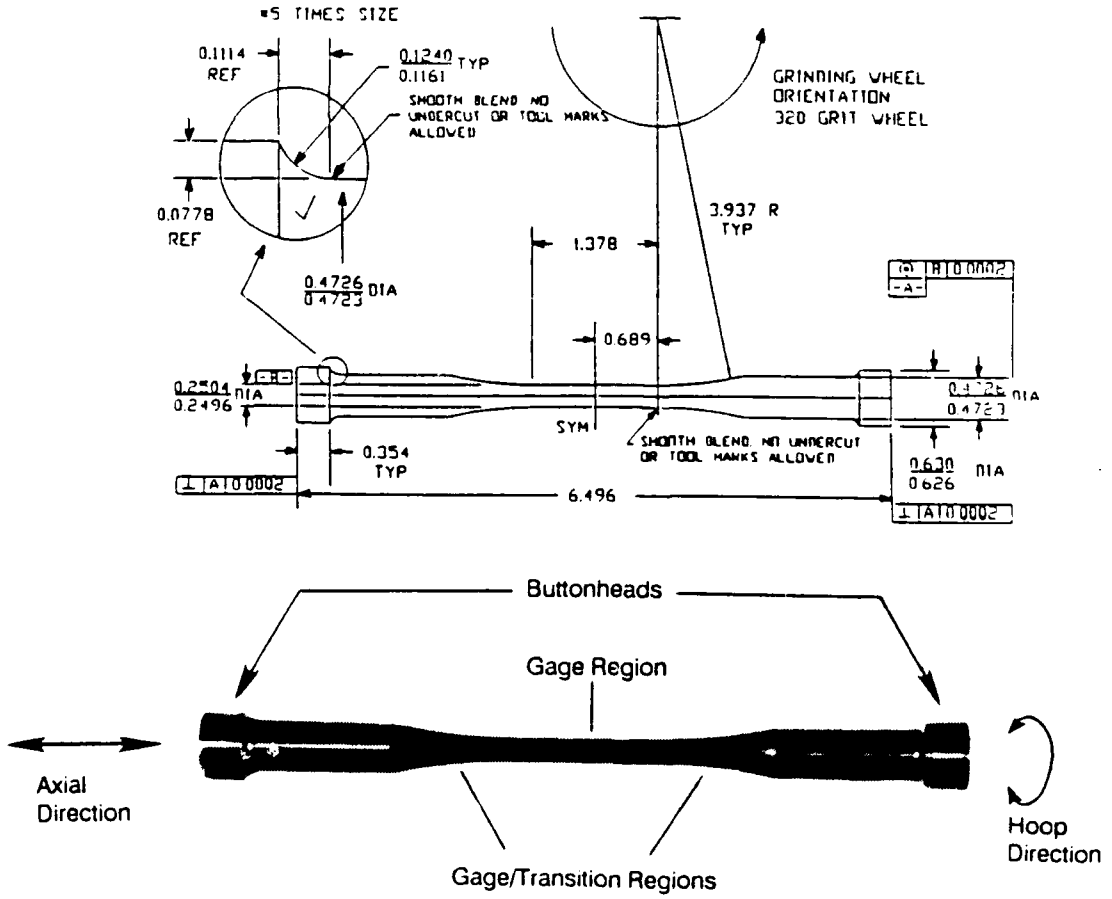

Figure 1. SG/NICC silicon nitride cylindrical buttonhead tensile specimen.

PRINCIPLES OF XRD RESIDUAL STRESS MEASUREMENT

X-ray diffraction is described by the Bragg law:

$$\eta\lambda = 2d \sin\theta \tag{1}$$

where:

- η = an integer (it is the order of reflection and usually equal to unity for residual stress determination)
- λ = wavelength of the incident radiation
- d = distance between parallel planes of atoms (d-spacing)
- θ = Bragg angle.

Diffraction from a crystalline material occurs when the Bragg relation is satisfied.

The principle of XRD residual stress measurement is based upon the fact that strain induced in a crystalline material as a consequence of mechanical deformation, phase transformation, thermal expansion, etc., causes a change in the spacing of the atomic planes within the crystal structure from that in the stress-free condition. This change in interatomic, or d-, spacing is evidenced as a shift in the diffracted X-ray peak position. By determining the angular peak shift and applying the Bragg law to quantify the d-spacing, the stress on the surface of a specimen can be calculated via linear elastic theory. Assuming that plane stress conditions exist on the surface; i.e., a biaxial system as illustrated in Figure 2, the relationship of interatomic strain to stress is given by

$$\varepsilon_{\phi\psi} = \left(\frac{1+\upsilon}{E}\right)\sigma_\phi \sin^2\psi - \frac{\upsilon}{E}(\sigma_1 + \sigma_2) \tag{2}$$

where

- $\varepsilon_{\phi\psi} = (d_{\phi\psi} - d_0)/d_0$ = strain in the direction defined by angles ϕ and ψ (d_0 is the interatomic spacing in the stress-free condition)
- E, υ = material elastic constants
- σ_ϕ = surface stress in the direction defined by angle ϕ
- ψ = angle between the surface normal and the normal to the crystallographic planes from which an X-ray peak is diffracted
- σ_1, σ_2 = principal stresses on the surface.

This equation is used to calculate the stress σ_ϕ in any direction on the surface of the specimen.

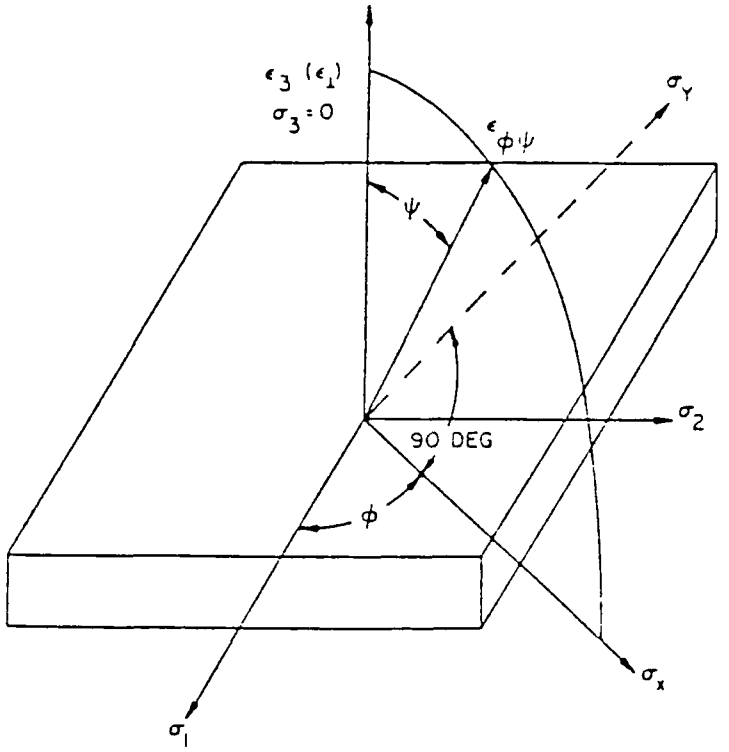

Figure 2. Biaxial stress system (from Reference 6).

Residual stress determined from diffracted X-rays represent strain averaged over a finite measurement volume comprised of the surface area irradiated by the X-ray beam and the depth to which it penetrates (typically, only a few tens of microns). When mechanical deformation processes, such as machining or grinding, induce uniform and continuous plastic strain in the surface layers of a material different from that in the bulk, the resultant residual stress is referred to as a macrostress. Plastic deformation nonuniformly distributed from grain to grain in a single-phase material or between matrix and precipitates in a multiphase system cause microresidual stresses to form. Macrostress is observed as a shift in X-ray peak position; microstress is exhibited in peak broadening and can be evaluated by full-width half-maximum values. The third type of residual stress is known as a pseudo-macrostress and describes average microstress within a sampled volume of grains. Pseudo-macrostresses are generated by rolling or drawing operations and also cause peak shifts that may influence the residual stress magnitude.[7,8] This investigation was concerned with the measurement and analysis of true surface macrostress produced by machining.

MTL has an advanced X-ray diffraction-based instrument capable of measuring residual stress in polycrystalline metals and ceramics. The Technology for Energy Corporation (TEC) Model 1610 X-Ray Stress Analysis System features a low power X-ray tube (100 watts, maximum) and a fixed location linear position-sensitive proportional counter (PSPC), and employs the $\sin^2 \psi$ stress measuring technique. The PSPC is a sealed gas detector that uses a 50 mm long carbon-coated quartz fiber wire anode for peak position encoding. At a specimen-to-detector distance (diffractometer radius) of 208.7 mm (8.2"), the PSPC subtends approximately

7. NOYAN, I. C. *Equilibrium Conditions for the Average Stresses Measured by X-Rays.* Metall. Trans. A., v. 14A, September 1983, p. 1907-1914.
8. CULLITY, B. D. *Some Problems in X-Ray Measurements.* Adv. in X-Ray Anal., v. 20, 1977, p. 251-279.

12^{o} of the instrument's diffraction angle 2θ range of 122^{o} to 166^{o}. Diffraction peaks in the high-back reflection region (2θ values approaching 180^{o}) are much preferred because they show the greatest angular shift sensitivity with a given amount of stress. The Model 1610 allows for the utilization of up to 10 ψ angles per stress measurement.

The $\sin^2 \psi$ technique requires a series of peak position measurements for a particular set of hkl planes be made at different tilts (ψ angles) of the crystallographic plane normal (see "N" in Figure 3) referenced to the normal of the specimen surface. The angular position of the diffracted peak is determined by least squares parabolic-curve fitting and used to calculate d-spacing from the Bragg relation. A plot is then constructed of d-spacing versus $\sin^2 \psi$, and the slope of a least squares line fitted to the experimental data multiplied by the X-ray elastic constant $E/(1+\upsilon)$ is proportional to the stress on the plane of the surface. The slope is found by differentiating Equation 2 with respect to $\sin^2 \psi$:

$$\text{slope} = [\partial\ (d_{\phi\psi} - d_o)/d_o]/[\partial\ \sin^2\psi]. \qquad (3)$$

A linear d-spacing versus $\sin^2 \psi$ plot (see Figure 4) indicates that the strain distribution is homogeneous within the irradiated volume[10] and that the assumption of a biaxial stress state is valid. Sin-square-psi plots that split into two branches (ψ-splitting) or exhibit curvature reveal a three-dimensional stress field containing pseudo-macro components of stress.

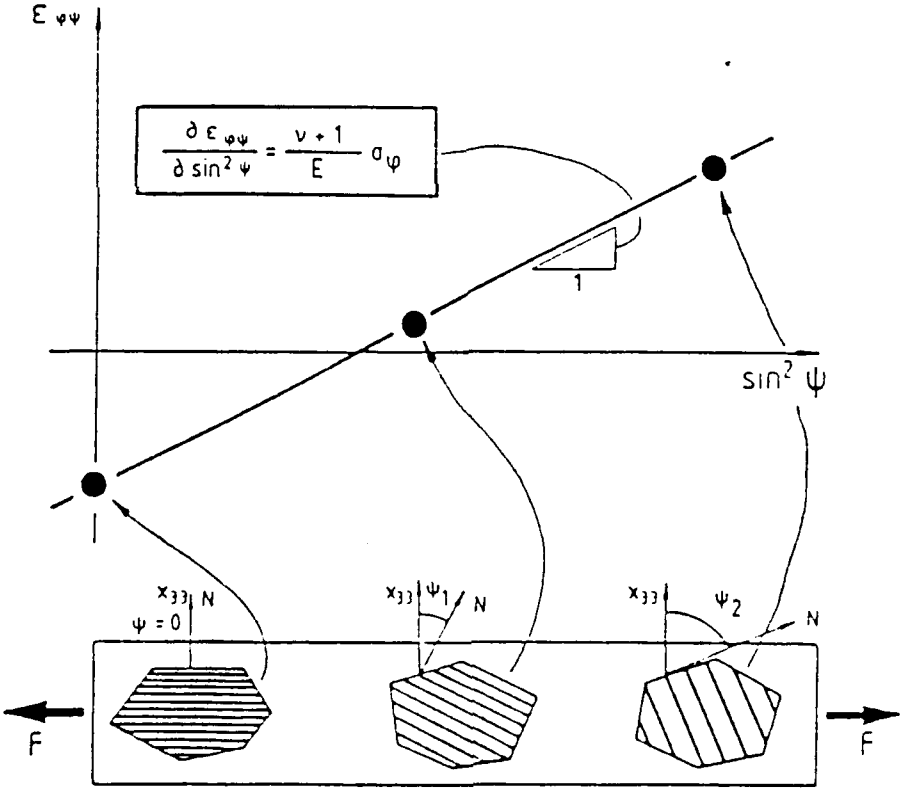

Figure 3. Schematic of the $\sin^2 \psi$ technique (from Reference 9).

9. EIGENMANN, B., SCHOLTES, B., and VOHRINGER, O. *Nondestructive Residual-Stress Analysis of Engineering-Ceramic Components with the Aid of X-Ray Stress Measurement*. Ceram. Forum Intl./Ber. DKG 66, no. 9, September 1989, p. 364-370.

10. NOYAN, I. C., and COHEN, J. B. *Residual Stress: Measurement by Diffraction and Interpretation*. Springer-Verlag, New York, NY, 1987, p. 161.

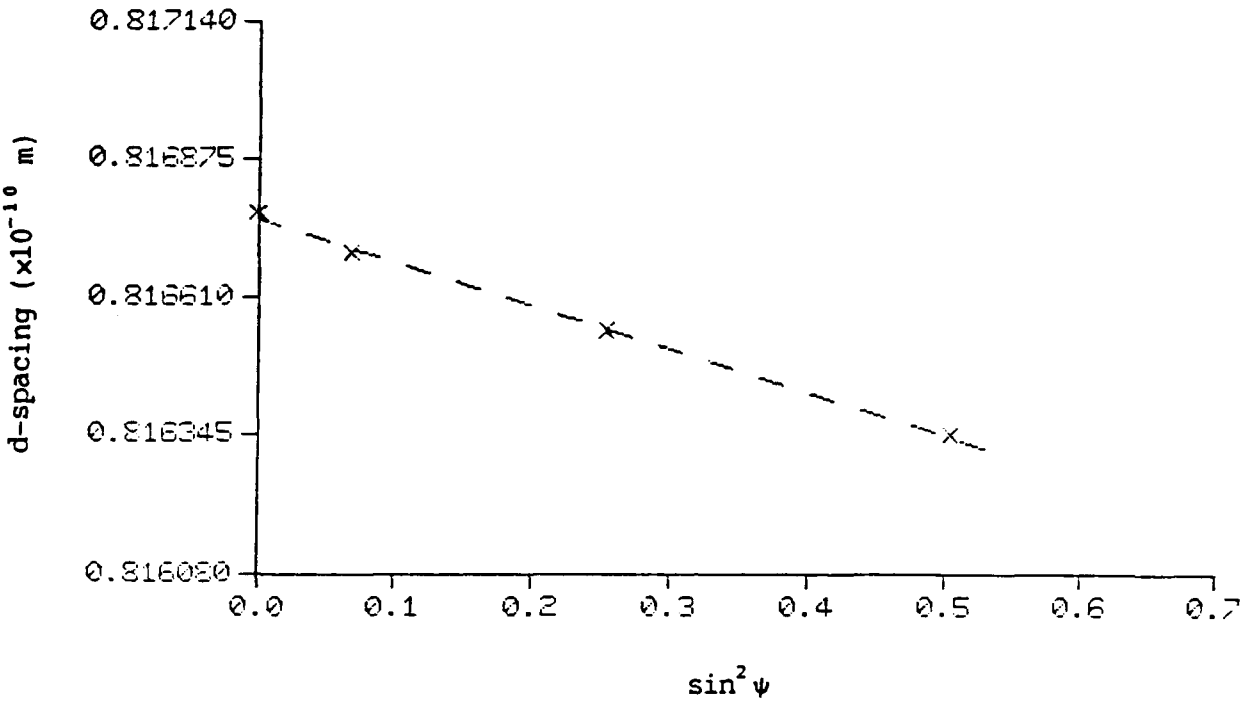

Figure 4. Plot of d-spacing versus $\sin^2\psi$ from a tensile rod specimen.

EXPERIMENTAL PROCEDURES

All silicon nitride residual stress measurement data were obtained from a four-positive ψ angle arrangement with copper K_α radiation diffracted from the (323) β-phase crystallographic planes at a nominal peak position of 141.5° 2θ. (James and Pardue[11] have recommended that only positive ψ angles be used with 2θ values less than 145° on divergent beam, fixed proportional counter residual stress analysis systems since negative ψ tilts cause large defocusing errors resulting in inaccurate peak location and subsequent calculated stress. However, to test for stress gradients normal to the surface due to shear stresses σ_{13} and σ_{23}, both positive and negative ψ angles are required. An alternative $\pm\ \psi$ setup for diffraction peaks less than 145° is achieved by first making a measurement using only + ψ angles and then rotating around the specimen normal 180° (while maintaining planar integrity) and remeasuring at the same location with the same + ψ values. Several finish-machined tensile rods were examined in this manner with no evidence of ψ-splitting; and the associated residual stress magnitudes were within one standard deviation of those determined from the four-positive ψ angle arrangement.) The incident X-ray beam was collimated to provide a 1 mm x 5 mm irradiated area on the surface of the cylindrical buttonhead tensile specimens with the short dimension in the direction of measurement for hoop stress determination. Axial residual stress measurements were performed on the tensile rods with the collimator turned 90° thereby placing the 5 mm dimension along the length of the specimen (see Figure 1 for hoop and axial stress directions). The collimators used for the fractured flexure bars and crushed buttonhead powder samples were 3 mm round and 1 mm x 5 mm, respectively. Figure 5 shows typical TEC diffraction spectra from β-phase silicon nitride.

11. JAMES, M. R., and PARDUE, E. B. S. *X-Ray Diffraction Focusing Circle Errors for a PSPC Based System*. ICRS-II, Nancy, France, November 23-25, 1988.

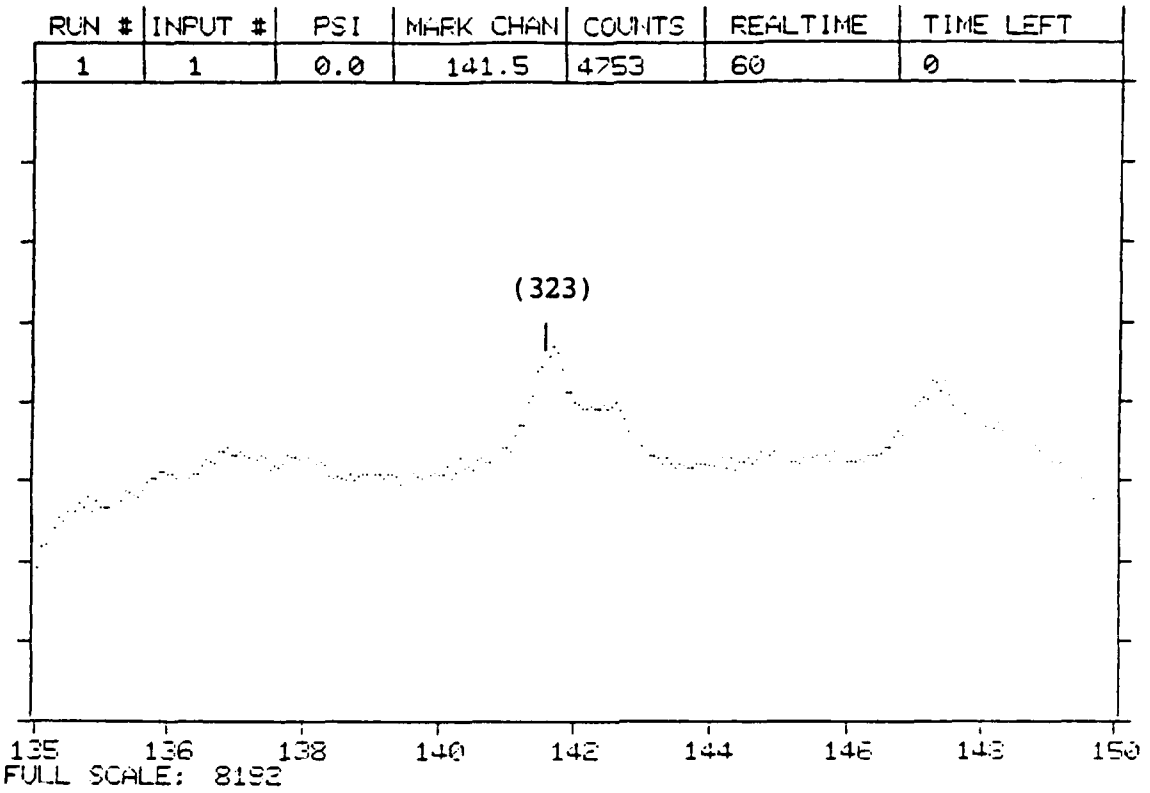

Figure 5. TEC diffraction spectra from β-phase silicon nitride.

The reported precision of measurement is the averaged total stress error values (root mean square of the counting and goodness of fit errors) generated for each measurement by the TEC error analysis software. Counting error results from the statistical nature of the X-rays counted by the detector, while the goodness of fit error is caused by diffraction peak asymmetrics due to polarization, absorption, and scattering effects. Accuracy is largely dependent upon the validity of the elastic constants used in calculating the stress magnitude and on the contribution from systematic errors. One such error, true ψ position, is encountered on curved-surface specimens. An estimate of less than 5% error for biaxial stress states has been given[12] when the ratio of the half width of the irradiated area to the specimen diameter is less than 0.13. For the cylindrical buttonhead tensile specimens, this ratio is 0.08.

When component geometry prevents the entire, normally-orientated beam (short dimension in the direction of measurement) from striking only the planar surface of interest, such as with the tensile rod axial direction measurements, rectangular collimators are sometimes rotated 90° to increase diffracted peak intensity. In doing so, however, spatial resolution is compromised insofar as the number of measurements that can be made in a given area (one versus five, in this case). Also, the affect on calculated stress values due to possible systematic error introduction must be resolved. To do this, the -117.5 ksi carbon steel stress standard supplied with the TEC system was used (with chromium radiation). The standard measured -122.8 ksi ± 6.2 ksi with the collimator normally oriented and -122.3 ksi ± 9.0 ksi when it was rotated. Disparity between the standard and the empirical residual stress

12. NOYAN, I. C., and COHEN, J. B. *Residual Stress: Measurement by Diffraction and Interpretation*. Springer-Verlag, New York, NY, 1987, p. 203.

values can be attributed to the fact that TEC established the standard's -117.5 ksi magnitude with a 4 mm round collimator (which averages stresses over a larger area than a 1 mm x 5 mm collimator) and with different data collection parameters than were used for this study. However, the tensile rod hoop and axial direction average total stress errors (± 3.8 ksi and ± 6.5 ksi, see Results and Discussion Section) are consistent with that from the TEC standard (± 6.2 ksi and ± 9.0 ksi). It is, therefore, concluded that any error introduced from true position deviation or collimator rotation is taken up in the overall precision of measurement.

An X-ray elastic constant $E/(1+\upsilon)$ of 260 GPa (37.7 x 10^6 psi) was utilized for all β-phase silicon nitride residual stress calculations. The modulus of elasticity, or Young's modulus E, and Poisson's ratio υ values of 330 GPa (47.9 x 10^6 psi) and 0.27, respectively, were taken from Reference 13. These were experimentally determined for the (323) reflections and may be different from bulk values which represent average elastic properties for all crystallographic directions. When analyzing residual stress in a multiphase material, only one phase is measured for a given set of crystallographic planes.

A fixture dedicated to support and orientate the tensile rod specimens is shown in Figure 6 along with the TEC *stresshead* (X-ray tube, detector, collimator, etc.) and partial-machined specimen R16. Table 2 summarizes the direction, orientation, and location of stress measurements on the tensile rods. In an attempt to characterize hot isostatic pressed (HIP)-related residual stresses, specimen R16 was machined off center axis in the gage region providing a nonmachined as-HIPed surface area (designated 0^o) and machined surfaces at four different depths of stock removal. The 0^o orientation was arbitrarily chosen on all other tensile rod specimens. The fractured flexure bars were measured only in the longitudinal direction at one location, the machined end on the SG/NICC designated tensive surface. Powder samples were prepared from crushed buttonheads according to standard diffraction pattern procedure.[14]

Table 2. RESIDUAL STRESS MEASUREMENT DIRECTIONS, ORIENTATIONS (AROUND), AND LOCATIONS ON THE TENSILE ROD SPECIMENS

Specimen(s)	Stress Measuring Direction	Orientation, Degrees	Location
1, 2, 3, 4	Axial	0, 90, 225	Center of Gage Region and Gage/Transition Region
1, 2	Hoop, Axial Axial	0, 90, 225 0, 90, 225	Center of Gage Region Gage/Transition Region
I27, I36	Hoop, Axial	0, 90	Center of Gage Region
D71	Hoop, Axial	0, 90	Center of Gage Region
NL, NT, N18, NI, NV	Hoop, Axial	0, 180	Center of Gage Region
R16	Hoop, Axial	0, 45, 90, 135, 180, 225, 270, 315	Center of Gage Region

13. PRÜMMER, R., and PFEIFFER-VOLLMAR, H. W. *Determination of Surface Stresses of High Temperature Ceramic Materials*. Proc. Brit. Ceram. Soc., 1984, p. 89-98.

14. KLUG, H. P., and ALEXANDER, L. E. *X-Ray Diffraction Procedures*. John Wiley & Sons, New York, NY, 1954, p. 193.

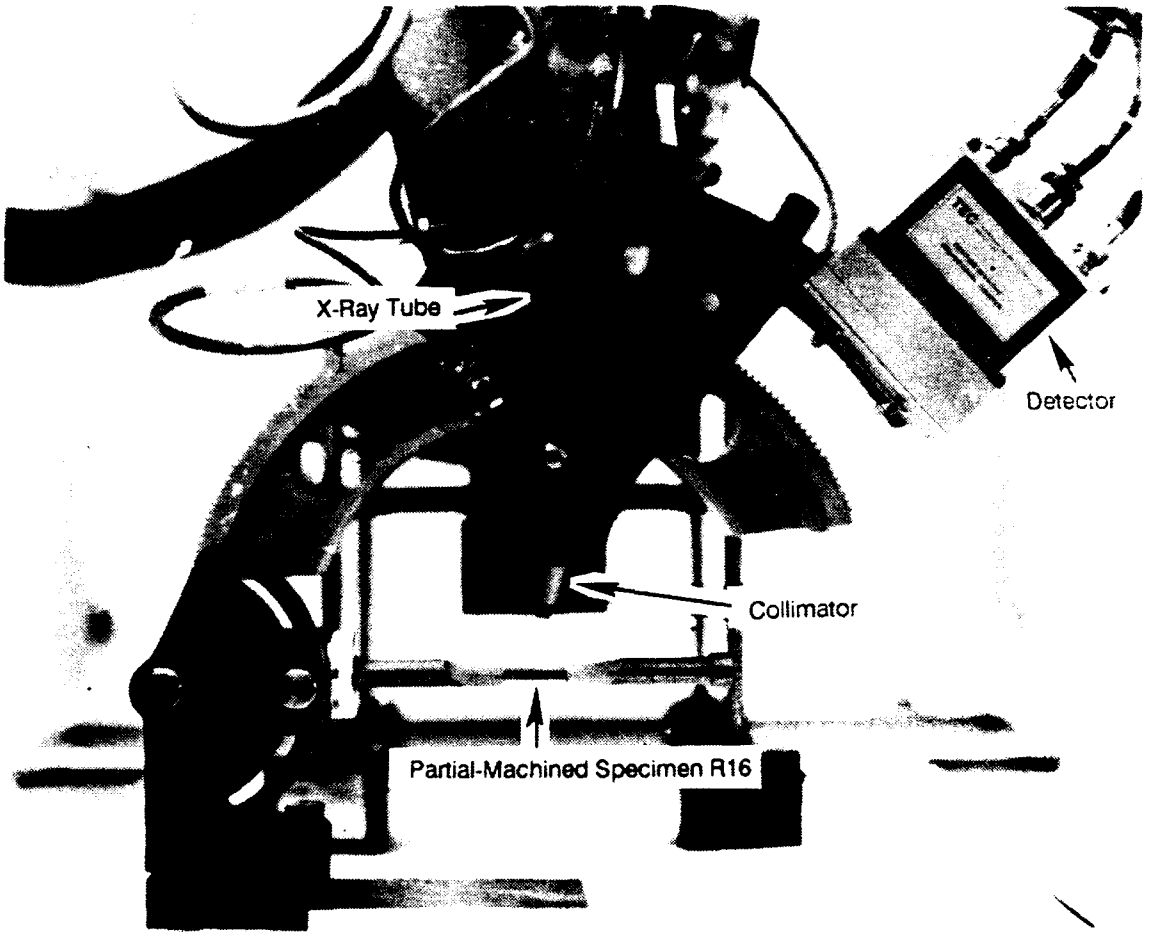

Figure 6. Tensile rod specimen support fixture and TEC stresshead.

The effective depth of penetration is obtained from an equation that relates the fraction of total diffracted intensity contributed by a surface layer to: (1) the depth of that surface layer, (2) the radiation-dependent linear absorption coefficient of the material, and (3) the sine of the Bragg angle.[15] A common way of reporting depth of penetration[16,17] is to calculate the depth of the surface layer from which 50% of the diffracted intensity originates. For copper radiation and the (323) planes of β-phase silicon nitride, the depth is 23 μm. An attempt at measuring residual stresses in a shallower near-surface layer was made using chromium radiation; however, only weak diffraction intensities (I/I_{max}) were observed in the stress analyzer's detectable 2θ range thus precluding accurate measurement.

15. CULLITY, B. D. *Elements of X-Ray Diffraction*. Addison-Wesley, Reading, MA, 2nd Edition, 1978, p. 292.
16. JOHNSON-WALLS, D., EVANS, A. G., MARSHALL, D. B., and JAMES, M. R. *Residual Stresses in Machined Ceramic Surfaces*. J. Am. Ceram. Soc., v. 69, no. 1, 1986, p. 44-47.
17. LANGE, F. F., JAMES, M. R., and GREEN, D. J. *Determination of Residual Surface Stresses Caused by Grinding in Polycrystalline Al_2O_3*. J. Am Ceram. Soc., v. 66, no. 2, C. 16-17, 1983.

RESULTS AND DISCUSSION

Tables 3 through 7 list residual stress and integrated intensity results from surface measurements performed on the tensile rod and flexure bar specimens. Negative residual stress values represent compressive stresses. The precision of measurement for the tensile rod specimens is ± 45 MPa (± 6.5 ksi) for axial direction data and ± 26 MPa (± 3.8 ksi) for the hoop direction. For the fractured flexure bars it is ± 37 MPa (± 5.4 ksi) and for the powder samples the precision is ± 26 MPa (± 3.8 ksi). Integrated intensity, taken from the area under the diffraction curve, is a relative measure of total diffracted energy for a given hkl plane, and is important as a means of detecting the presence and severity of preferred orientation in a specimen. It may also be used for comparative analysis of specimens that exhibit differing amounts of surface oxidation, reaction layer thickness, or when incomplete phase transformation is suspected.

Table 3. RESIDUAL STRESS FROM COLD ISOSTATIC PRESSED AND HIP FINISH-MACHINED TENSILE ROD SPECIMENS BEFORE AND AFTER HEAT TREATMENT

Specimen	Orientation, Degrees	Residual Stress, MPa (ksi) (Before)	(After)
	Axial Direction, Center of Gage Region		
1	0	-285 (-41.4)	-266 (-38.6)
	90	-262 (-38.0)	-262 (-38.0)
	225	-276 (-40.0)	-276 (-40.1)
2	0	-233 (-33.8)	-211 (-30.6)
	90	-178 (-25.8)	-207 (-30.0)
	225	-225 (-32.6)	-215 (-31.2)
3	0	-260 (-37.8)	
	90	-201 (-29.2)	
	225	-252 (-36.5)	
4	0	-235 (-34.1)	
	90	-243 (-35.3)	
	225	-270 (-39.2)	
	Hoop Direction, Center of Gage Region		
1	0		81 (11.8)
	90		45 (6.5)
2	0		46 (6.6)
	90		98 (14.8)
	Axial Direction, Gage/Transition Region		
1	0	-234 (-34.0)	-230 (-33.3)
	90	-287 (-41.6)	-241 (-34.9)
	225	-259 (-37.6)	-287 (-41.6)
2	0	-228 (-33.1)	-281 (-40.7)
	90	-239 (-34.7)	-274 (-39.7)
	225	-169 (-24.5)	-241 (-34.9)
3	0	-289 (-41.9)	
	90	-221 (-32.0)	
	225	-232 (-33.7)	
4	0	-191 (-27.1)	
	90	-234 (-34.0)	
	225	-207 (-30.0)	

Table 4. RESIDUAL STRESS AND INTEGRATED INTENSITY FROM INJECTION MOLDED AND HIP TENSILE ROD SPECIMENS

Specimen	Stress Measuring Direction	Orientation, Degrees	Residual Stress, MPa (ksi)	Integrated Intensity @ $\psi = 0^{o}$
		Center of Gage Region		
I27	Axial	0	-246 (-35.7)	180.0
		90	-223 (-32.4)	177.6
	Hoop	0	29 (4.2)	203.6
		90	45 (6.5)	204.6
I36	Axial	0	-234 (-34.0)	185.7
		90	-244 (-35.4)	185.7
	Hoop	0	61 (8.9)	205.6
		90	46 (6.7)	204.4
D71	Axial	0	-190 (-27.6)	256.2
		90	-210 (-30.4)	263.3
	Hoop	0	-76 (-11.0)	287.8
		90	-88 (-12.8)	296.0

Table 5. RESIDUAL STRESS AND INTEGRATED INTENSITY FROM PRESSURE CAST AND HIP FINISH-MACHINED TENSILE ROD SPECIMENS BEFORE AND AFTER HEAT TREATMENT

Specimen	Orientation, Degrees	Residual Stress, MPa (ksi) (Before)	Residual Stress, MPa (ksi) (After)	Integrated Intenstiy @ $\psi = 0^{o}$ (Before)	Integrated Intenstiy @ $\psi = 0^{o}$ (After)
		Axial Direction, Center of Gage Region			
NL	0	-303 (-43.9)	-315 (-45.7)	251.7	268.3
	180	-337 (-48.9)	-374 (-54.3)	259.2	256.7
NT	0	-344 (-49.9)	-366 (-53.1)	268.9	277.8
	180	-339 (-49.2)	-339 (-49.2)	249.1	260.4
N18	0	-303 (-43.9)	-324 (-47.0)	242.9	269.1
	180	-346 (-50.2)	-299 (-43.3)	279.6	279.4
NI	0	-291 (-42.2)	-388 (-56.3)	233.3	262.1
	180	-339 (-49.2)	-364 (-52.8)	261.6	266.1
NV*	0	-381 (-55.3)		186.4	
	180	-344 (-49.9)		167.6	
		Hoop Direction, Center of Gage Region			
NL	0	31 (4.5)	-6 (-0.8)	280.4	291.6
	180	35 (5.1)	36 (5.2)	275.7	276.9
NT	0	-3 (-0.5)	6 (0.8)	293.7	312.2
	180	14 (2.0)	31 (4.5)	277.8	282.6
N18	0	2 (0.3)	3 (0.5)	283.8	283.2
	180	-3 (-0.4)	17 (2.4)	287.2	294.7
NI	0	40 (5.8)	11 (1.6)	262.6	268.6
	180	19 (2.8)	-3 (-0.5)	288.4	294.2
NV*	0	-69 (-10.0)		198.5	
	180	-35 (-5.1)		190.4	

*Not heat treated.

Table 6. RESIDUAL STRESS AND INTEGRATED INTENSITY FROM PRESSURE CAST AND HIP PARTIAL-MACHINED TENSILE ROD SPECIMEN R16

Orentation, Degrees	Machining Depth, Inches	Residual Stress, MPa (ksi)	Integrated Intensity @ $\psi = 0^o$
		Axial Direction, Center of Gage Region	
0	0	*	61.4
45	0.012	-422 (-61.2)	180.0
90	0.048	-386 (-56.0)	250.9
135	0.104	-339 (-49.2)	249.3
180	0.114	-444 (-64.4)	285.1
225	0.104	-368 (-53.3)	255.0
270	0.048	-352 (-51.0)	227.3
315	0.012	-365 (-53.0)	172.4
		Hoop Direction, Center of Gage Regioin	
0	0	48 (6.9)	107.4
45	0.012	-28 (-4.0)	227.7
90	0.048	15 (2.2)	289.9
135	0.104	2 (0.3)	298.8
180	0.114	49 (7.1)	323.9
225	0.104	54 (7.9)	285.8
270	0.048	23 (3.3)	250.0
315	0.012	1 (0.2)	139.8

*Poor peak intensity due to β-phase deficient reaction layer prohibited accurate calculation.

Table 7. RESIDUAL STRESS AND INTEGRATED INTENSITY FROM FRACTURED FLEXURE BAR SPECIMENS

Specimen		Residual Stress, MPa (ksi)	Integrated Intensity @ $\psi = 0^o$
C005	#16	-27 (-3.9)	121.4
	#22	-78 (-11.3)	169.4
	#44	-25 (-3.6)	80.6
C006	#15	-14 (-2.0)	129.0
	#22	17 (2.5)	196.9
	#38	-29 (-4.2)	167.2
	#44	-2 (-0.3)	63.9
C007	#16	-8 (-1.2)	164.7
	#22	-2 (-0.3)	107.7
	#38	-33 (-4.8)	120.2
	#44	-23 (-3.4)	101.9
C008	#16	-6 (-0.8)	114.5
	#22	-59 (-8.6)	219.3
	#43	-42 (-6.1)	102.5

Cylindrical Buttonhead Tensile Specimens

Cold Isostatic Pressed and HIP

The axial direction residual stress measurement results from the finish-machined tensile rod specimens 1, 2, 3, and 4 listed in Table 3, independent of orientation and location, are uniform, averaging -238 ± 33 MPa (-34.5 ksi ± 4.8 ksi). These numbers agree reasonably well with other published machining induced surface residual stress data determined by the curvature method.[18] Tensive hoop stresses averaging 67 MPa ± 27 MPa (9.8 ksi ± 3.9 ksi) were measured on specimens 1 and 2 after heat treatment at the gage region center. Hoop direction measurements were not performed prior to heat treatment. Subjecting specimen 1 to heat treat "A" and specimen 2 to heat treat "B" (proprietary treatments) effected little change on the average gage region center axial direction residual stress values as shown in Figure 7. The pre-heat treatment residual stress difference between specimens 1 and 2 may reflect a slight variation in forming and densification parameters.

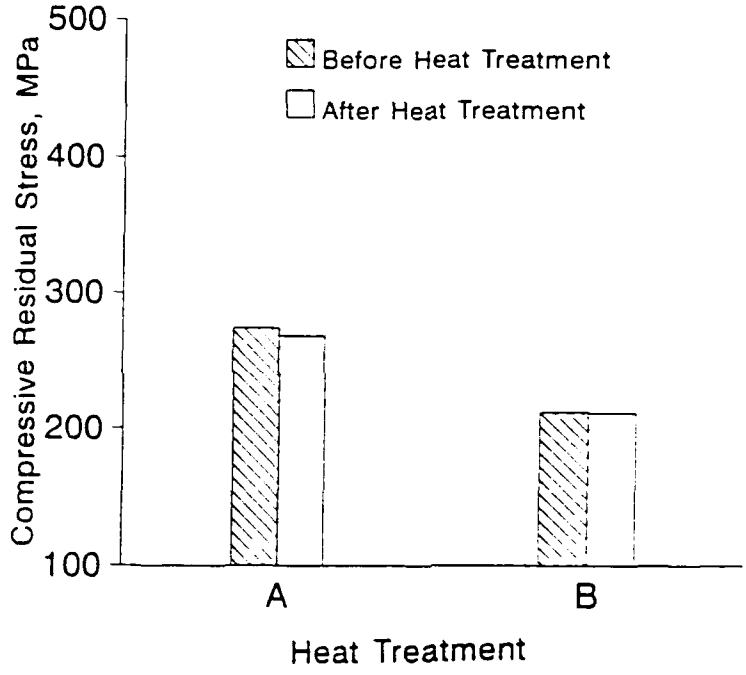

Figure 7. Heat treatment comparison of tensile rod axial direction residual stress.

Injection Molded and HIP

Zero and 90° axial direction residual stresses (see Table 4) measured at the center of the gage region are uniform and equivalent in magnitude and sign to the stresses measured on the cold isostatic pressed tensile rods. Hoop direction stresses are tensive on the "I" specimens and compressive on specimen D71. This may be attributed to the fact that the hoop stresses measured on the "I" specimens are machining induced, whereas those measured on the as-HIPed surface of the D71 specimen are related to the forming and densification processes. The larger integrated intensity values (indicative of a greater amount of converted β-phase Si_3N_4) from the D71 specimen when compared to the "I" specimens are probably due to the dissimilar "I" and "D" batch processing histories (proprietary).

18. SAMUEL, R., CHANDRASEKAR, S., FARRIS, T. N., and LICHT, R. H. *Effect of Residual Stresses on the Fracture of Ground Ceramics.* J. Am. Ceram. Soc., v. 72, no. 10, 1989, p. 1960-1966.

Pressure Cast and HIP

- Specimens NL, NT, N18, NI, and NV: Axial and hoop direction gage region residual stresses listed in Table 5 are approximately uniform both before (as-finish machined) and after heat treatment. No significant difference in average axial direction residual stress is noted between specimens from the three machine shops as shown in Figure 8. Variations in integrated intensities between the 0^{o} (arbitrarily chosen) and the 180^{o} orientations may indicate the existence of green body density gradients inherent to the casting process. (Independent research at SG/NICC has observed density gradients in the green body when formed by pressure casting.[19] This density gradient manifests itself into residual stresses in the final densified rod and causes warpage of the rod in the as-HIPed condition.) Specimen NV was subjected to a HIP temperature profile different than the other batch "N" specimens, therefore, the amount of converted β-phase would also be expected to differ. This is exhibited in the 30% variation in the respective mean integrated intensity values.

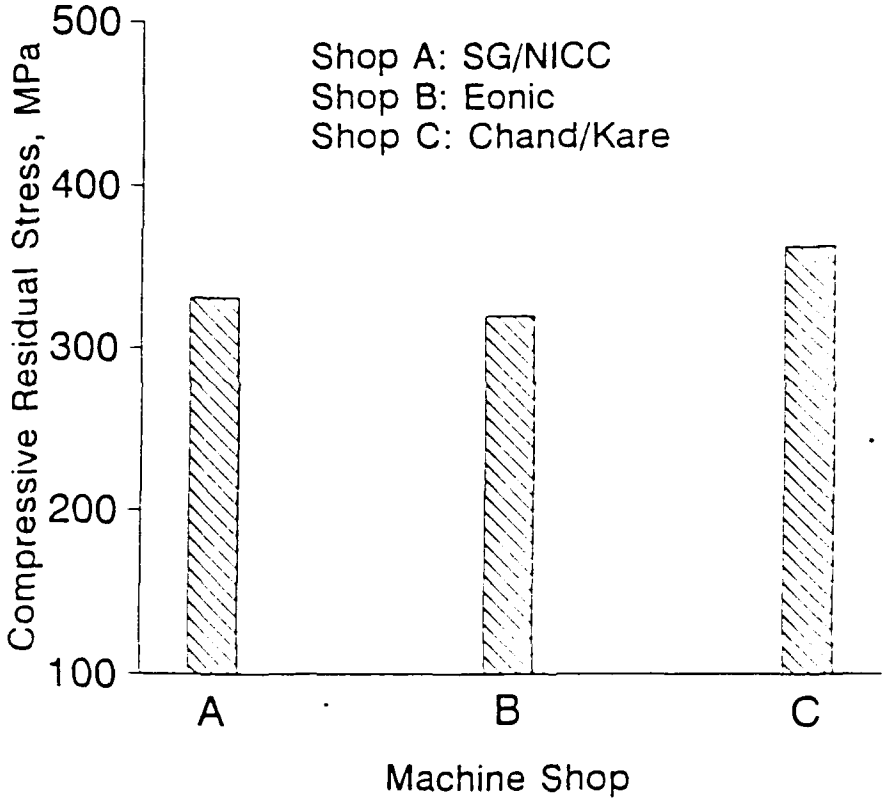

Figure 8. Machine shop comparison of tensile rod axial direction residual stress.

The average axial direction compressive residual stresses measured on the tensile rods produced by three distinct forming methods and all machined at shop "A" are displayed in Figure 9. While the residual stresses from the cold isostatic pressed and injection molded forming methods are roughly equivalent, the pressure cast specimens show a somewhat greater stress magnitude due to the density gradient described above.

19. FOLEY, M. R., et al. *Reliability Improvements of High Strength Silicon Nitride Through Process Optimization and Control.* Annual Automotive Technology Development Contractors Coordination Meeting, Dearborn, MI, October 28-31, 1991.

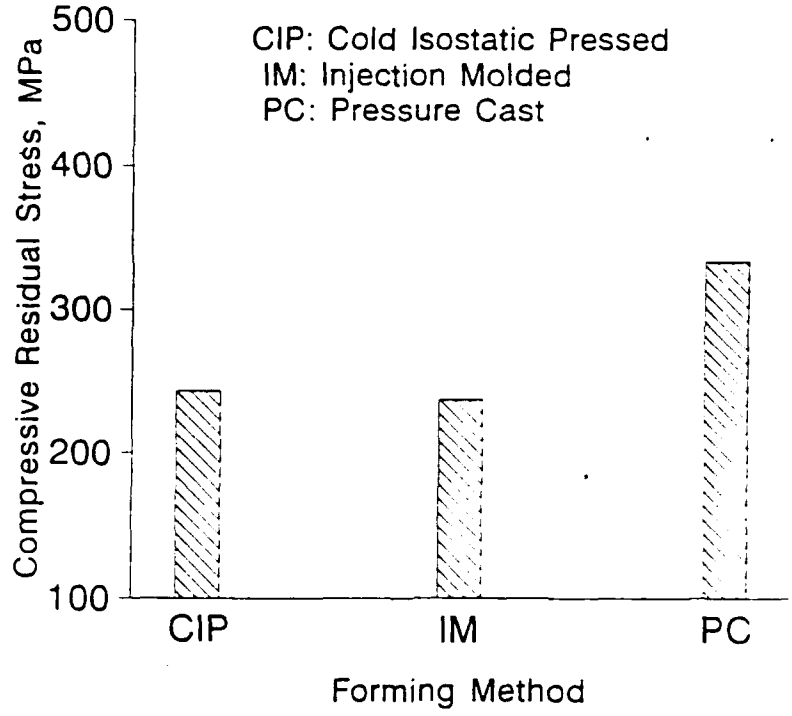

Figure 9. Forming method comparison of tensile rod axial direction residual stress.

- Specimen R16: The results of measurements performed at eight orientations corresponding to the four different depths of machining (0.012" at 45° and 315°, 0.048" at 90° and 270°, 0.104" at 135° and 225°, and 0.114" at 180°) and the nonmachined as-HIPed surface area (0°) are listed in Table 6. Both axial and hoop direction residual stresses are uniform around the specimen with the average axial compressive stress equal in magnitude to the "N" specimens and the average hoop stress being slightly more tensive. The semicircular trace of axial direction integrated intensity values in Figure 10 indicates a proportional increase in amount of β-phase as the HIP reaction layer is removed. The 45° and 315° measurement locations show a three-fold intensity gain with little material machined off (0.012"); the 180° location, at which the most material was removed (0.114"), yields the maximum intensity. It is foreseeable that X-ray diffraction integrated intensity data could be used as a quality control tool for the nondestructive assessment of reaction layer removal by machining.

Fractured Flexure Bar Specimens

The residual stress values listed in Table 7 average -23 MPa ± 25 MPa (-3.4 ksi ± 3.6 ksi), and are consistent with silicon nitride rectangular bar stress data from another investigation.[20] A uniform surface stress of this magnitude existing over the length of an unfractured flexure bar should have little effect on mechanical properties such as strength and toughness. Measurements were not performed on these specimens prior to fracture. The variation in the integrated intensity between the specimens is probably due to processing differences.

20. RUUD, C. O., and SNOHA, D. J. *Investigation of Residual Stresses in Structural Ceramic Components.* Final Report, U.S. Army Contract No. DAAG46-83-K-0036, U.S. Army Materials Technology Laboratory, Watertown, MA, September 1987, p. 40-56.

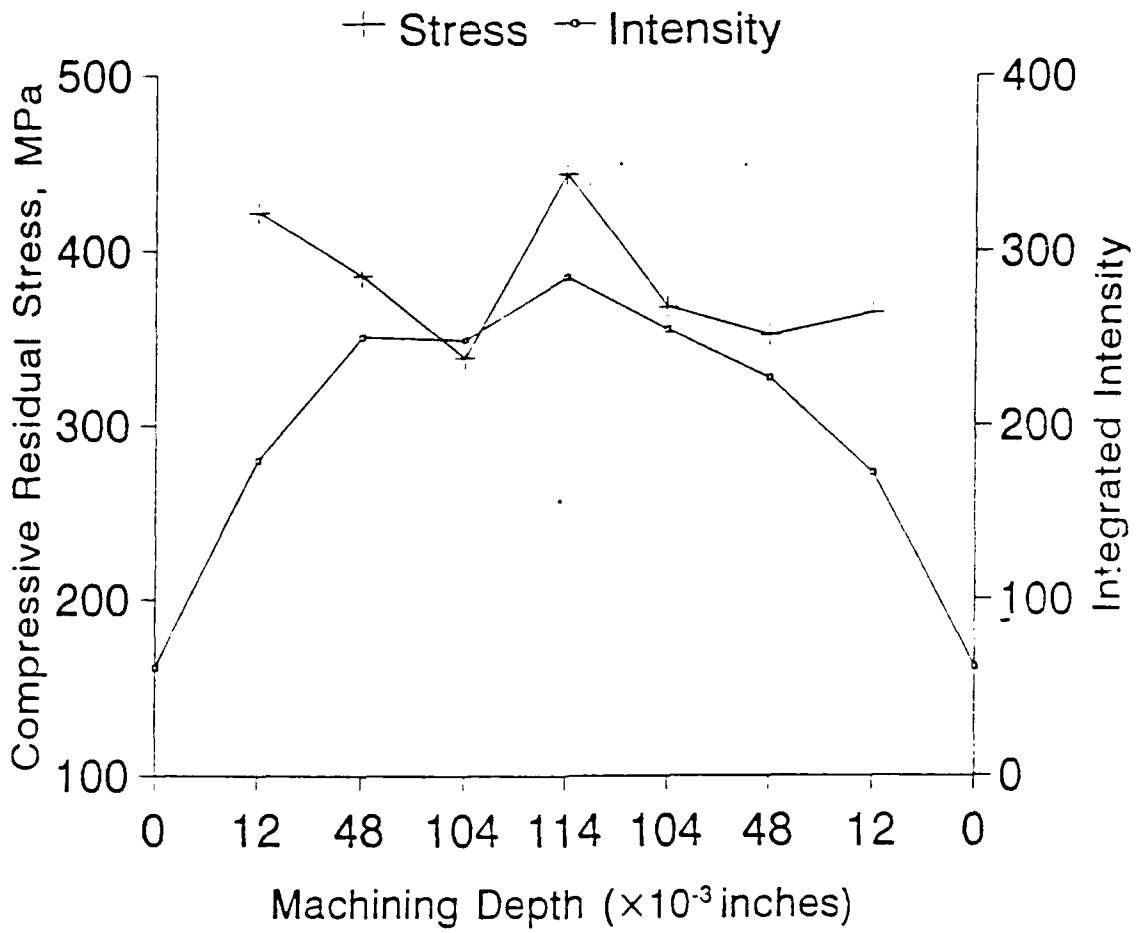

Figure 10. Axial direction residual stress and integrated intensity results from tensile rod specimen R16.

Crushed Buttonhead Powder Samples

Since a powder will not support a macro-residual stress between the loose particles, the tensive stresses measured on the T-end and 1-end crushed buttonhead powder samples, 70 MPa ± 26 MPa (10.1 ksi ± 3.8 ksi) and 99 MPa ± 27 MPa (14.4 ksi ± 3.9 ksi), respectively, were thought to be anomalous results. To determine if displacement or alignment errors biased these data, and unannealed -325 mesh 99.8% magnesium powder (AESAR Lot #18529) was measured in accordance with ASTM Standard E 915-85 (Verifying the Alignment of X-Ray Diffraction Instrumentation for Residual Stress Measurement). Magnesium powder was chosen because copper K_α radiation diffracts from the (214) crystallographic planes at 141.0° 2θ (almost identical to the (323) β-phase Si_3N_4 diffraction angle, see Experimental Procedures Section) and both materials have hexagonal structures. With the same data collection parameters as used throughout this investigation, the magnesium powder measured an ASTM acceptable 8 MPa ± 10 MPa (1.1 ksi ± 1.4 ksi) suggesting that the contribution of systematic errors is minimal. However, this result is somewhat misleading because the X-ray elastic constant $E/(1+\upsilon)$ of magnesium is approximately one-eighth that of β-phase silicon nitride (35 GPa[21] compared to 260 GPa). And since the residual stress magnitude is

21. FINK, D. G., and McKENZIE, A. A., eds., *Electronics Engineers Handbook*. McGraw-Hill, New York, NY, 1st Edition, 1975, p. 6-12.

directly related to the elastic constant (through the slope of the $\sin^2\psi$ plot), slight systematic or material-related inconsistencies will be more prominent in the ceramic powder data. Other factors could also have contributed to the measured T-end and 1-end powder residual stresses. For example, the powders were produced by crushing the buttonheads of tensile rod specimen NT and, therefore, were made up of a mixture of particles from the surface layer as well as from bulk material. It is likely that the crystal structure, second-phase composition, microstrain condition, and/or size of these particles varied throughout the powder samples. Cullity,[22] in his section on particle size effects, has indicated that individual crystals less than about 0.1 μm will cause peak broadening. Comparing the average full-width, half-maximum (FWHM) value from the crushed buttonhead powders (1.42°) to that from specimen NT prior to crushing (1.24°, and typical of all tensile rod FWHM values), implies that this effect may have occurred. The FWHM from the magnesium powder was 0.89°.

Powder diffraction quantitative phase analysis was performed on the crushed buttonhead powder samples at SG/NICC, and a good correlation was found between these results and MTL residual stress measurement integrated intensity values. For the T-end powder, the percentage of β-phase Si_3N_4 was determined to be 81.7, and the integrated intensity value (averaged from five measurements) was 221.9 for a ratio of 0.368. The 1-end powder β-phase quantity to integrated intensity ratio was 88.4 to 248.0 or 0.357.

CONCLUSIONS

No significant difference in residual stress was observed on the pressure cast tensile rods that were machined at three different shops.

Axial residual stress was 30% greater on the pressure cast tensile rods when compared to cold isostatic pressed or injection molded rods. Hoop stresses were approximately equivalent for all forming methods.

The post-machining heat treatments utilized in this investigation had virtually no effect on residual stress.

Integrated intensity of the β-phase increased proportionally with the amount of stock removed on the partial-machined tensile rod specimen.

Residual stress was negligible on the machined surface of the fractured flexure bar specimens.

Powder diffractometer quantitative phase analysis results compared well with residual stress analyzer integrated intensity data on the crushed buttonhead powder samples.

ACKNOWLEDGMENTS

The authors wish to extend appreciation to Mr. Ray Hinxman of MTL and Mr. Anil Parmar of SG/NICC for their powder diffraction work.

22. CULLITY, B. D. *Elements of X-Ray Diffraction*. Addison-Wesley, Reading, MA, 2nd Edition, 1978, p. 284.

DISTRIBUTION LIST

No. of Copies	To
1	Office of the Under Secretary of Defense for Research and Engineering, The Pentagon, Washington, DC 20301
	Commander, U.S. Army Laboratory Command, 2800 Powder Mill Road, Adelphi, MD 20783-1145
1	ATTN: AMSLC-IM-TL
1	AMSLC-CT
	Commander, Defense Technical Information Center, Cameron Station, Building 5, 5010 Duke Street, Alexandria, VA 22304-6145
2	ATTN: DTIC-FDAC
1	MIA/CINDAS, Purdue University, 2595 Yeager Road, West Lafayette, IN 47905
	Commander, Army Research Office, P.O. Box 12211, Research Triangle Park, NC 27709-2211
1	ATTN: Information Processing Office
	Commander, U.S. Army Materiel Command, 5001 Eisenhower Avenue, Alexandria, VA 22333
1	ATTN: AMCSCI
	Commander, U.S. Army Materiel Systems Analysis Activity, Aberdeen Proving Ground, MD 21005
1	ATTN: AMXSY-MP, H. Cohen
	Commander, U.S. Army Missile Command, Redstone Scientific Information Center, Redstone Arsenal, AL 35898-5241
1	ATTN: AMSMI-RD-CS-R/Doc
1	AMSMI-RLM
	Commander, U.S. Army Armament, Munitions and Chemical Command, Dover, NJ 07801
2	ATTN: Technical Library
	Commander, U.S. Army Natick Research, Development and Engineering Center, Natick, MA 01760-5010
1	ATTN: Technical Library
	Commander, U.S. Army Satellite Communications Agency, Fort Monmouth, NJ 07703
1	ATTN: Technical Document Center
	Commander, U.S. Army Tank-Automotive Command, Warren, MI 48397-5000
1	ATTN: AMSTA-ZSK
1	AMSTA-TSL, Technical Library
	Commander, White Sands Missile Range, NM 88002
1	ATTN: STEWS-WS-VT
	President, Airborne, Electronics and Special Warfare Board, Fort Bragg, NC 28307
1	ATTN: Library
	Director, U.S. Army Ballistic Research Laboratory, Aberdeen Proving Ground, MD 21005
1	ATTN: SLCBR-TSB-S (STINFO)
	Commander, Dugway Proving Ground, UT 84022
1	ATTN: Technical Library, Technical Information Division
	Commander, Harry Diamond Laboratories, 2800 Powder Mill Road, Adelphi, MD 20783
1	ATTN: Technical Information Office
	Director, Benet Weapons Laboratory, CWSL, USA AMCCOM, Watervliet, NY 12189
1	ATTN: AMSMC-LCB-TL
1	AMSMC-LCB-R
1	AMSMC-LCB-RM
1	AMSMC-LCB-RP
	Commander, U.S. Army Foreign Science and Technology Center, 220 7th Street, N.E., Charlottesville, VA 22901-5396
3	ATTN: AIFRTC, Applied Technologies Branch, Gerald Schlesinger
	Commander, U.S. Army Aeromedical Research Unit, P.O. Box 577, Fort Rucker, AL 36360
1	ATTN: Technical Library

No. of Copies	To
	Commander, U.S. Army Aviation Systems Command, Aviation Research and Technology Activity, Aviation Applied Technology Directorate, Fort Eustis, VA 23604-5577
1	ATTN: SAVDL-E-MOS
	U.S. Army Aviation Training Library, Fort Rucker, AL 36360
1	ATTN: Building 5906-5907
	Commander, U.S. Army Agency for Aviation Safety, Fort Rucker, AL 36362
1	ATTN: Technical Library
	Commander, USACDC Air Defense Agency, Fort Bliss, TX 79916
1	ATTN: Technical Library
	Commander, Clarke Engineer School Library, 3202 Nebraska Ave., N, Ft. Leonard Wood, MO 65473-5000
1	ATTN: Library
	Commander, U.S. Army Engineer Waterways Experiment Station, P.O. Box 631, Vicksburg, MS 39180
1	ATTN: Research Center Library
	Commandant, U.S. Army Quartermaster School, Fort Lee, VA 23801
1	ATTN: Quartermaster School Library
	Naval Research Laboratory, Washington, DC 20375
1	ATTN: Code 5830
2	Dr. G. R. Yoder - Code 6384
	Chief of Naval Research, Arlington, VA 22217
1	ATTN: Code 471
1	Edward J. Morrissey, WRDC/MLTE, Wright-Patterson Air Force Base, OH 45433-6523
	Commander, U.S. Air Force Wright Research & Development Center, Wright-Patterson Air Force Base, OH 45433-6523
1	ATTN: WRDC/MLLP, M. Forney, Jr.
1	WRDC/MLBC, Mr. Stanley Schulman
	NASA - Marshall Space Flight Center, MSFC, AL 35812
1	ATTN: Mr. Paul Schuerer/EH01
	U.S. Department of Commerce, National Institute of Standards and Technology, Gaitherburg, MD 20899
1	ATTN: Stephen M. Hsu, Chief, Ceramics Division, Institute for Materials Science and Engineering
1	Committee on Marine Structures, Marine Board, National Research Council, 2101 Constitution Avenue, N.W., Washington, DC 20418
1	Materials Sciences Corporation, Suite 250, 500 Office Center Drive, Fort Washington, PA 19034-3213
1	Charles Stark Draper Laboratory, 68 Albany Street, Cambridge, MA 02139
	Wyman-Gordon Company, Worcester, MA 01601
1	ATTN: Technical Library
	General Dynamics, Convair Aerospace Division P.O. Box 748, Forth Worth, TX 76101
1	ATTN: Mfg. Engineering Technical Library
	Plastics Technical Evaluation Center, PLASTEC, ARDEC Bldg. 355N, Picatinny Arsenal, NJ 07806-5000
1	ATTN: Harry Pebly
1	Department of the Army, Aerostructures Directorate, MS-266, U.S. Army Aviation R&T Activity - AVSCOM, Langley Research Center, Hampton, VA 23665-5225
1	NASA - Langley Research Center, Hampton, VA 23665-5225
1	U.S. Army Propulsion Directorate, NASA Lewis Research Center, 2100 Brookpark Road, Cleveland, OH 44135-3191
1	NASA - Lewis Research Center, 2100 Brookpark Road, Cleveland, OH 44135-3191
	Director, U.S. Army Materials Technology Laboratory, Watertown, MA 02172-0001
2	ATTN: SLCMT-TML
2	Authors

U.S. Army Materials Technology Laboratory
Watertown, Massachusetts 02172-0001
AN INVESTIGATION OF RESIDUAL STRESSES IN MACHINED SILICON NITRIDE -
Daniel J. Snoha and Michael R. Foley

AD__________
UNCLASSIFIED
UNLIMITED DISTRIBUTION

Key Words

Residual stress
X-ray diffraction
Silicon nitride

Technical Report MTL TR 92-46, July 1992, 20 pp-
illus-tables,

An X-ray diffraction (XRD) residual stress investigation was conducted on groups of machined silicon nitride specimens utilizing copper Kα radiation, the (323) β-phase crystallographic planes and the $\sin^2 \psi$ stress-measuring technique. Cylindrical buttonhead tensile specimens formed by different processes and finish machined by different shops were characterized both before and after heat treatment. Surface machining stresses were also determined on a partial-machined tensile rod and on fractured flexure bars. The residual stress results are presented in the form of a comparative evaluation of processing parameters. Supplemental integrated intensity data from measurements on the partial-machined tensile rod and crushed buttonhead powder samples has demonstrated that XRD residual stress analysis may be applicable as a quality assurance procedure.

U.S. Army Materials Technology Laboratory
Watertown, Massachusetts 02172-0001
AN INVESTIGATION OF RESIDUAL STRESSES IN MACHINED SILICON NITRIDE -
Daniel J. Snoha and Michael R. Foley

AD__________
UNCLASSIFIED
UNLIMITED DISTRIBUTION

Key Words

Residual stress
X-ray diffraction
Silicon nitride

Technical Report MTL TR 92-46, July 1992, 20 pp-
illus-tables,

An X-ray diffraction (XRD) residual stress investigation was conducted on groups of machined silicon nitride specimens utilizing copper Kα radiation, the (323) β-phase crystallographic planes and the $\sin^2 \psi$ stress-measuring technique. Cylindrical buttonhead tensile specimens formed by different processes and finish machined by different shops were characterized both before and after heat treatment. Surface machining stresses were also determined on a partial-machined tensile rod and on fractured flexure bars. The residual stress results are presented in the form of a comparative evaluation of processing parameters. Supplemental integrated intensity data from measurements on the partial-machined tensile rod and crushed buttonhead powder samples has demonstrated that XRD residual stress analysis may be applicable as a quality assurance procedure.

U.S. Army Materials Technology Laboratory
Watertown, Massachusetts 02172-0001
AN INVESTIGATION OF RESIDUAL STRESSES IN MACHINED SILICON NITRIDE -
Daniel J. Snoha and Michael R. Foley

AD__________
UNCLASSIFIED
UNLIMITED DISTRIBUTION

Key Words

Residual stress
X-ray diffraction
Silicon nitride

Technical Report MTL TR 92-46, July 1992, 20 pp-
illus-tables,

An X-ray diffraction (XRD) residual stress investigation was conducted on groups of machined silicon nitride specimens utilizing copper Kα radiation, the (323) β-phase crystallographic planes and the $\sin^2 \psi$ stress-measuring technique. Cylindrical buttonhead tensile specimens formed by different processes and finish machined by different shops were characterized both before and after heat treatment. Surface machining stresses were also determined on a partial-machined tensile rod and on fractured flexure bars. The residual stress results are presented in the form of a comparative evaluation of processing parameters. Supplemental integrated intensity data from measurements on the partial-machined tensile rod and crushed buttonhead powder samples has demonstrated that XRD residual stress analysis may be applicable as a quality assurance procedure.

U.S. Army Materials Technology Laboratory
Watertown, Massachusetts 02172-0001
AN INVESTIGATION OF RESIDUAL STRESSES IN MACHINED SILICON NITRIDE -
Daniel J. Snoha and Michael R. Foley

AD__________
UNCLASSIFIED
UNLIMITED DISTRIBUTION

Key Words

Residual stress
X-ray diffraction
Silicon nitride

Technical Report MTL TR 92-46, July 1992, 20 pp-
illus-tables,

An X-ray diffraction (XRD) residual stress investigation was conducted on groups of machined silicon nitride specimens utilizing copper Kα radiation, the (323) β-phase crystallographic planes and the $\sin^2 \psi$ stress-measuring technique. Cylindrical buttonhead tensile specimens formed by different processes and finish machined by different shops were characterized both before and after heat treatment. Surface machining stresses were also determined on a partial-machined tensile rod and on fractured flexure bars. The residual stress results are presented in the form of a comparative evaluation of processing parameters. Supplemental integrated intensity data from measurements on the partial-machined tensile rod and crushed buttonhead powder samples has demonstrated that XRD residual stress analysis may be applicable as a quality assurance procedure.